

Mesoporous Carbon/Co₃O₄ Hybrid as Efficient Electrode for Methanol Electrooxidation in Alkaline Conditions

D.K. Hassan¹, S.A. El-safty^{2,3}, Khalil Abdelrazek Khalil^{1,4,*}, M. Dewidar¹, G. Abu el-maged⁵

¹Mechanical Design and Materials Department, Faculty of Energy Engineering, Aswan University, Aswan 81521, Egypt

²National Institute for Materials Science (NIMS), Research Center for Strategic Materials, 1-2-1 Sengen, Tsukuba-shi, Ibaraki-ken, 305-0047, Japan

³Graduate School of Advanced Science and Engineering, Waseda University, 3-4-1 Okubo, Shinjuku-Ku, Tokyo, 169-8555, Japan

⁴King Saud University, Department of Mechanical Engineering, College of Engineering, P.O. Box 800, Riyadh 11421, Saudi Arabia

⁵Mechanical Design and Production Department, Faculty of Engineering, Minia University, El-Minia, Egypt

*E-mail: kabdelmawgoud@ksu.edu.sa

Received: 27 June 2016 / Accepted: 4 August 2016 / Published: 6 September 2016

Controlling the combined features of electroactive materials to achieve remarkable improvements in all aspects of electrochemical performances is a great challenge. In this report, C/Co₃O₄ micro-spherical flowers were directly grown on three dimensional (3-D) porous nickel foam (NF) via a facile microwave-assisted hydrothermal approach followed by a post-annealing process. The self supported structure was employed in the electrocatalytic oxidation of methanol. Impressively, the hybrid C/Co₃O₄ electrode exhibits outstanding electrocatalytic activity and superior stability towards methanol electrooxidation compared to that of pristine Co₃O₄ fabricated by similar procedure. The higher reactivity of the mesoporous hybrid C/Co₃O₄ is largely attributed to the synergetic contribution of both carbon matrices and Co₃O₄ electroactive sites. Furthermore, the enhanced electronic configuration of the hybrid is mainly due to carbon embedment which greatly facilitates the electron transport in the electrode and further promotes the reaction kinetics. Results indicate that the conductive nickel substrate supported the binder free C/Co₃O₄ electrode can be considered as a potential candidate for high-performance energy storage and conversion devices and meet the desired features of high electrocatalytic activity and long-term stability which is indispensable for direct methanol fuel cells.

Keywords: Cobalt oxide, composite materials, direct growth, energy storage and conversion.

1. INTRODUCTION

The fast-growing needs for green, cost effective, and efficient energy systems have aroused widespread attentions over the past decades [1-3]. Direct methanol fuel cells (DMFCs) have been

considered as one of the most potential energy storage devices owing to their preferable features including higher energy density, low toxicity, and lower operating cost [4,5]. Although, platinum based electrocatalyst are the most attractive electrocatalysts for DMFCs due to their excellent catalytic activity. However, their expensive cost and limited sources hinder the large-scale commercialization of DMFCs [6-8]. In addition, platinum catalysts are readily poisoned by the intermediate during the reaction which is an additional obstacle for their practical application in DMFCs [9]. To realize a broad application of DMFCs, a great progress has been performed to improve the performance fuel cells in terms of electrode systems by applying new low cost, efficient, and durable electroactive materials [10,11]. The development of novel electroactive materials is emerged as an effective way to enhance the efficiency of DMFCs and to substitute or even reduce the utilization of platinum-based electrocatalysts [9-11].

To date, nanostructured metal oxides and their hybrids have stimulated considerable research interest to improve the performance of DMFCs due to their synergistic characteristics of high surface area, enhanced catalytic activity, and improved electronic configuration [12,13]. Interestingly, these metal oxides have received considerable attentions due to their comparatively low preparation cost, earth abundance, and improved features with respect to chemical stability as well as resistance to poisoning [14]. Among those active metal oxides, Co_3O_4 based electrodes have received a significant deal of attention due to their lower fabrication cost and higher electrocatalytic activity [15-18]. Previous reports have been demonstrated that composite materials display promising catalytic activities better than individual components [19]. Therefore, numerous efforts are underway with regard to promote the reactivity metal oxide based catalysts [20]. It is well accepted that carbon supports such as carbon black, carbon nanotubes, and graphene can effectively improve the electrical conductivity of transition metal oxides [16,20].

Hierarchical porous nanostructures with large surface area and controlled morphology have emerged as a promising solution to substitute the current commercial electrode materials because of their sophisticated features including fast electron transport, short ion diffusion, and sufficient contact between the electrolyte and electroactive materials [21,22]. Various synthetic routes have been developed to explore electroactive nanostructures with different surface morphologies and fascinating micro/nanostructures [23-25]. However, special protocols are required to fabricate heterostructured electrocatalytic materials with high activity and superior structural stability. Up until now, the direct growth of electroactive species on conductive substrates has generated huge interest due to the favorable features and multifunctionalities offered by this synthetic approach. The absence of binders or polymeric additives can improve the kinetic of electron transfer at the electrode/electrolyte interfaces and greatly enhance the electrical conductivity of the active materials [19,26-28].

The fabrication of Co_3O_4 nanostructures with tunable morphology is a key factor for further improvement of nanostructured cobalt oxides. Along with this, hybrids heterostructures composed of Co_3O_4 and carbon support can offer special characteristics and advantages better than individual component through a direct modification of each other.

Recently, the electrocatalysis of methanol oxidation reaction of cost-effective catalysts has been receiving growing attentions [12,19]. However, the design and synthesis of mesoporous hybrid electrocatalysts with unique structural features and the electro-activities of each component are fully

manifested is still poorly understood. Transition metal oxides like nanoparticles or films structures are commonly prepared using conventional routes related to established large-scale industrial syntheses. Our work aims to change this direction.

With special emphasis on the advancements, little research has been afforded to utilize 3-D hierarchical structures grown directly on porous substrate for methanol oxidation in alkaline conditions. This study unravels the synergetic role of direct growth of electroactive materials with extraordinary properties which could potentially aid in the future design of new strategic electrocatalysts.

In this work, C/Co₃O₄ hybrid was directly synthesized on a conductive 3-D porous nickel substrate with robust adhesion using a cost effective one-pot hydrothermal approach. The carbon species were successfully embedded into the integrated architecture under the addition of thiourea as a capping agent for the fabrication of flower-like structures. After a sequential conversion from the precursor C/Co(CO₃)_{0.5}(OH)·0.11H₂O in air, C/Co₃O₄ micro-spherical flowers were obtained. The free standing composite electrode was applied as anode materials for methanol electrooxidation in alkaline conditions. Our findings demonstrate that the enhanced electrochemical performances of the binder-free electrode can be ascribed to (i) the direct contact of catalytic material to the current collector reduces the ion diffusion resistance and greatly enhance the electronic features, (ii) the well-defined mesoporous structure facilitate the diffusion of chemical species into mesopores, and (iii) the absence of polymeric binders improve the electrical conductivity and significantly increase the exposed electroactive surfaces leading to better utilization of the catalytic material. Results indicate that our proposed synthesis strategy can guide the design of highly electroactive materials for practical applications in electrochemical energy devices and catalysts.

2. EXPERIMENTAL SECTION

2.1. Materials and chemicals

Cobalt chloride hexahydrate (CoCl₂·6H₂O) and thiourea CH₄N₂S were purchased from Wako Co., Ltd., Osaka, Japan. 2,6-diaminopurine as well as the commercial nickel foams were obtained from Tokyo Industry Company (TCI). All the chemicals were of analytical grade and used without further modifications.

2.2. Synthesis

3-D porous NF was investigated as a substrate to grow the target material directly on its skeletons. Before investigation, the as-received NF was cleaned by sonication in concentrated HCl solution for 20 min. After that, the substrate was rinsed thoroughly in methanol, Milli-Q water, and then dried overnight. To fabricate carbon supported Co₃O₄ micro-spherical flowers (C/Co₃O₄), 2,6-diaminopurine was used as a carbon source. Typically, 0.2 M CoCl₂·6H₂O and 1 M of CH₄N₂S were dissolved in 40 mL of deionized water by stirring until a clear pink solution was obtained. 120 mg of 2,6-diaminopurine was added to the solution under vigorous stirring to form a homogenous mixture.

The obtained reaction mixture was transferred into a 75 mL Teflon liner and then a cleaned NF tailored into (2cm*2cm) was inserted into the mixture parallel to the reaction autoclave. The top side of NF was isolated with polytetrafluoroethylene tape to prevent contamination. The liner with the reaction mixture was sealed and exposed to microwave irradiation (600 W) for 1 h at 160 °C before cooling down to room temperature. The resulting NF immobilized with the active material was washed with deionized methanol and water several times and dried under vacuum at 60 °C for 8 h. The precursor was annealed at 350 °C for 4 h to produce C/Co₃O₄ micro-spherical flowers. For comparison, pure Co₃O₄ was synthesized by the same method.

2.3. Material characterization

The morphologies and surface structures of the hybrid C/Co₃O₄ and Co₃O₄ micro-spherical flowers were observed on field emission scanning electron microscopy (FE-SEM, JEOL model 6500) operated at 15 kV to ensure high resolution micrographs. In addition, high-resolution transmission electron microscopy and energy dispersive spectroscopy (STEM-EDS) were performed using a JEOL JEM model 2100F microscope operated at 200 kV accelerating voltage. The active material was dispersed on ethanol to form a clear solution, dropped into a copper grid, and then dried in air before further investigations. The crystal structure and composition of the samples were characterized by X-ray diffraction (XRD) patterns using Bruker D8 Advance diffractometer with Cu_{Kα}-X-radiation and wavenumber of $\lambda = 1.54178 \text{ \AA}$. The recorded diffraction patterns were investigated by DIFRAC plus Evaluation Package (EVA) software provided by Bruker AXS. The Raman spectrum was carried out on Raman spectroscopy (Horiba, JobinYvon) using an excitation laser source of 533 nm wavelength. The spectrum was analyzed by LabSpec-3.01C software. The N₂ adsorption/desorption isotherms were measured using a BELSORP36 (JP. BEL Co., Ltd.) analyzer at 77 K. The samples were thermally treated under N₂ flow at 200 °C for 6 h. The surface area was measured by Brunauer-Emmett-Teller (BET) method and the corresponding pore size distribution was measured using the nonlocal density functional theory (NLDFT).

2.4. Electrochemical investigation

The electrochemical performances of the electrodes were measured in a traditional three electrode cell using platinum wire ($\Phi=0.1 \text{ mm}$) and mercury/mercury oxide (Hg/HgO, M NaOH) as the counter and reference electrode, respectively. NF modified with the active materials was investigated as the working electrodes. The electrocatalytic performances of self supported electrodes were collected in 0.5 M KOH by cyclic voltammetry (CV), chronoamperometry (CA), and electrochemical impedance spectroscopy (EIS) tests using a Zennium/ZAHNER work station (Elektrik GmbH & Co. KG). The electrocatalytic activity of the electrode for methanol oxidation was evaluated in 0.5 M KOH with 0.5 M methanol. Prior to measurements, the electrolyte was bubbled with a steady N₂ stream for 30 min and maintained above the solution during the experiment to attain N₂-saturated electrolyte. The EIS measurements were carried out in the frequency range from 100 kHz to 10 mHz at

the open circuit potential. In addition the stability test was performed using chronoamperometry test at a fixed potential of 0.55 V (vs. Hg/HgO) in presence of 0.5 M methanol for 7200 s.

3. RESULTS AND DISCUSSION

3.1 Synthesis and construction of flower-like architecture

Controlling the morphological structure and composition of electroactive materials can efficiently enhance their electrocatalytic activities. Herein, we successfully fabricate C/Co₃O₄ on 3-D porous NF using one-pot microwave-assisted hydrothermal method as schematically illustrated in Fig. 1. Simply, the precursor was produced by dissolving cobalt chloride hexahydrate and thiourea in water followed by the addition of carbon source. The resulting mixture with NF was then loaded into an autoclave before hydrothermal treatment under microwave irradiation.

Subsequently, the precursors were subjected to microwave irradiation at relatively low temperature to form a uniform layer of cobalt carbonate hydroxide on the microporous scaffolds of the NF electrodes. The as-obtained precursor was carefully annealed under air flow at the peak temperature to produce the final product named C/Co₃O₄ micro-spherical flowers.

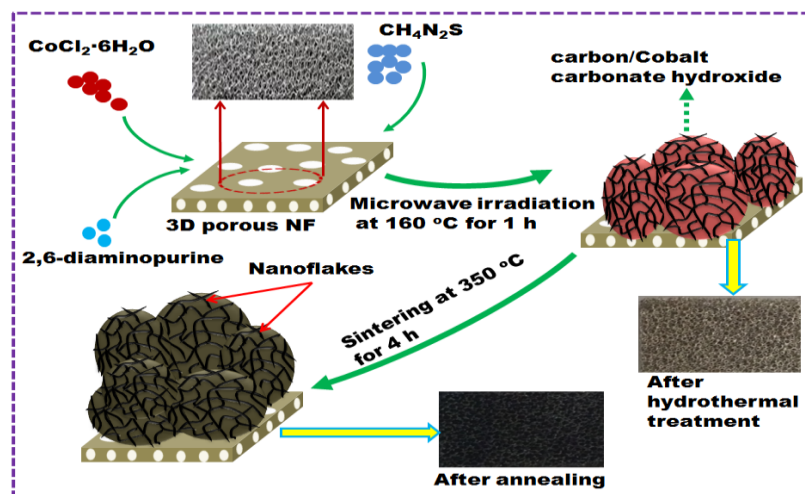


Figure 1. Representative illustration of the synthesis procedure using one-pot microwave-assisted hydrothermal approach. The reactants were subjected to microwave irradiation for 1 h at 160 °C to grow a homogeneous film of the composite on the NF skeleton and then annealed under air flow to produce C/Co₃O₄-NF electrode.

The urea was investigated as an auxiliary reagent to successfully grow Co-based nanostructures on a conductive substrate. The formed composed of a large number of multidirectional nanoflakes with the diameter ranging from 2-4 μm . Notably, the hydrolysis of urea ions led to the creation of CO₃²⁻ and OH⁻ which subsequently interact with the Co species to produce Co(OH)_x(CO₃)_{0.5}·0.11H₂O precipitate. The obtained precursor was then decomposed to the final product C/Co₃O₄ via a simple annealing process. Additionally, during the thermal treatment of reactants, the crystal growth of Co₃O₄ particles

might occur via the aggregation of Co precursor which facilitates the formation of the engineered structure at low surface energy. Together, the electrostatic binding between the hydroxyl groups of cobalt carbonate and the surface group of the carbon source lead to preferable growth of Co nuclei during the assemble of dendritic nanoflakes. This clearly indicates that the preparation process of Co flower-like architecture is mostly consistent with the previously reported by Jing Kong et al [29] which involve the nucleation of primary particles and followed by attachment and crystallization of these particles.

3.2 Physical characterization

The wide-angle powder X-ray diffraction spectra (WA-XRD) (Fig. 2) show that the Co particles were preferably rearranged and the observed diffraction can be indexed as face-centered cubic phase of Co_3O_4 ($Fd\bar{3}m$, JCPDS 42-1467) [30,31]. The weak peak detected at $2\Theta \sim 25.3^\circ$ is attributed to the (200) reflection of carbon [32]. This finding indicates that the carbon keep the characteristic features of single cubic Co_3O_4 and enhance crystal structure stability.

The sharp and narrow diffraction peaks indicate good crystallinity of the prepared materials which is possibly attributed to well-controlled synthesis process and compatible hydrothermal environment for the growth of Co crystals. The grains size was measured according to the Debye – Scherrer equation [33]:

$$d = (0.94 \lambda)/(\beta \cos\theta) \quad (1)$$

Where d is the average crystalline grain size, λ is the wavelength ($\lambda = 1.542 \text{ \AA}$), β is the function width at half maximum (FWHM) of the line, and θ is the diffraction angle. Results show that the grain size of the as-synthesized C/ Co_3O_4 was measured to be $\sim 32 \text{ nm}$.

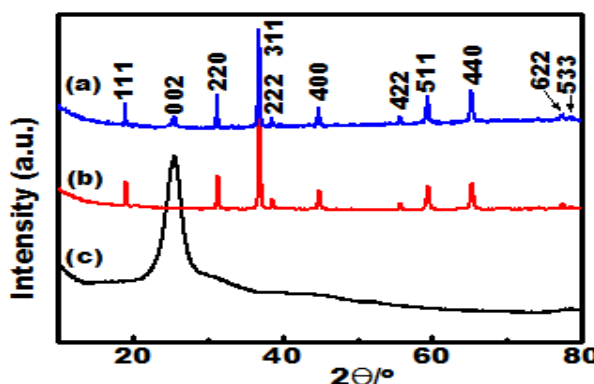


Figure 2. XRD patterns of the samples scratched down from the substrate; (a) C/ Co_3O_4 , (b) Co_3O_4 , and (c) carbon.

The Raman spectra were investigated to further illustrate the composition of the as-synthesized materials as depicted in Fig. 3. The Raman pattern of the composite C/ Co_3O_4 shows four distinctive peak located at 484 , 528.2 , 621.5 and 685 cm^{-1} assigned to E_g , F_{2m}^1 , F_{2g}^2 and A_{1g} vibrational modes of Co_3O_4 [34,35]. While, the broad peaks detected at 1356.5 and 1575 cm^{-1} named as D-band and G-band,

respectively, are attributed to the A_{1g} and E_{2g} vibration modes of the embedded carbon atoms [36]. The integral intensity ratio of the D/G band (I_D/I_G) is an indication to the degree of graphitization which is beneficial for the electronic configuration of Co_3O_4 nanoparticles. Results show that the relative intensity ratio I_D/I_G was measured to be 1.1 and 1.04 for the hybrid C/ Co_3O_4 and graphitic carbon, respectively.

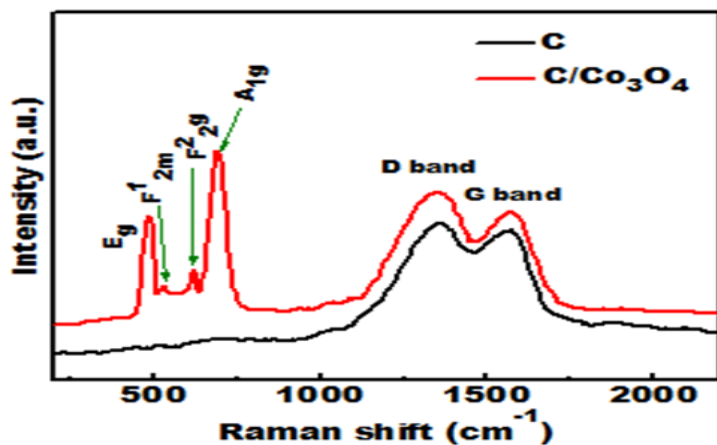


Figure 3. Raman spectra of pure carbon nanoparticles and mesoporous hybrid C/ Co_3O_4

3.3 Morphology and surface structure

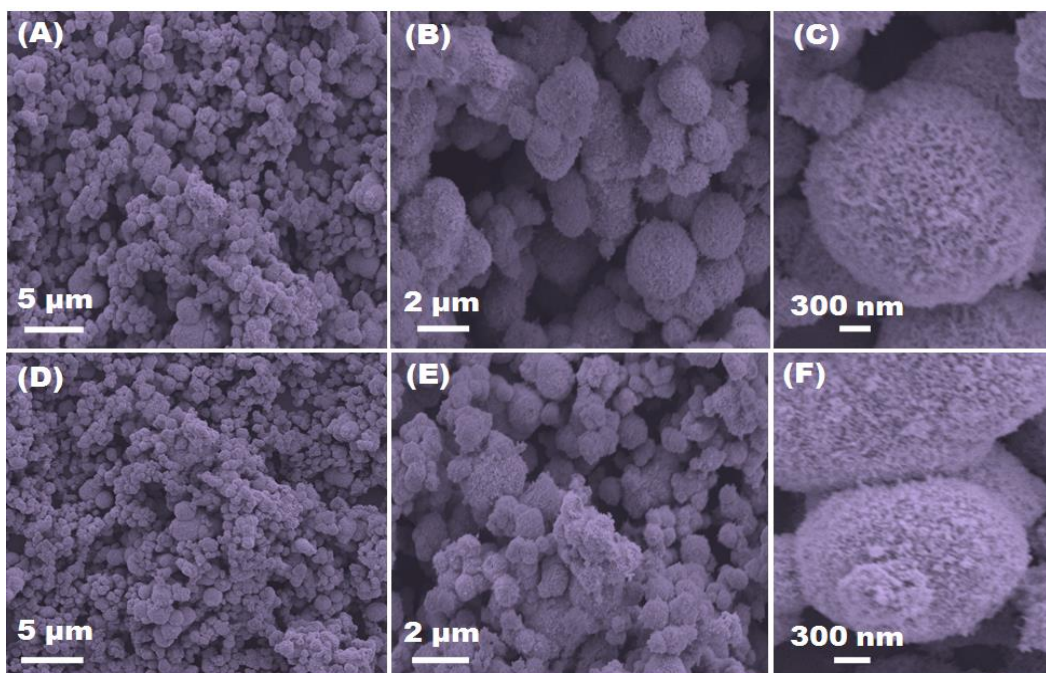


Figure 4. FE-SEM observations of the electrodes viewed at different magnifications of mesoporous Co_3O_4 (A–C) and C/ Co_3O_4 hybrid (D–F).

The surface morphology and size of the synthesized samples were initially investigated via SEM (Fig. 4A–F). Clearly, the obtained flower-like structures were assembled from numerous

interconnected nanoflakes with an average thickness of 50-80 nm. The size of the hierarchical mesoporous flower-like structure might be increased gradually due to the self attachment of nanoflakes (petals) on their surfaces. Interestingly, the morphology of the engineered flower-like structure was well preserved after loading the carbon source nanoparticles demonstrating higher stability of the integrated flower-like architectures (Fig. 4D–F). The open hierarchical texture in the C/Co₃O₄ micro-spherical flowers as well as the porous structure may enable fast electron transport and significantly facilitate the penetration of reactant molecules and be easily absorbed onto the electroactive sites as well as the pore network matrices of the building structure [37,38].

The TEM profiles of the porous hybrid (Fig. 5A–C) show that the carbon particles were homogenously distributed through the whole structure and along the nanoflakes. Obviously, the produced flower-like architectures were seemed to be assembled from a solid interior core with numerous helically arranged nanoflakes growing on it and further evidencing the formation of C/Co₃O₄ micro-spherical flowers. A closer observation of TEM images further reveal a well-developed porous structure within the hierarchical morphology. The high magnification TEM image of a microflower (Figure 5C) reveals a large number of pores within the structure which might act like ion reservoirs for high performance electrochemical reactions.

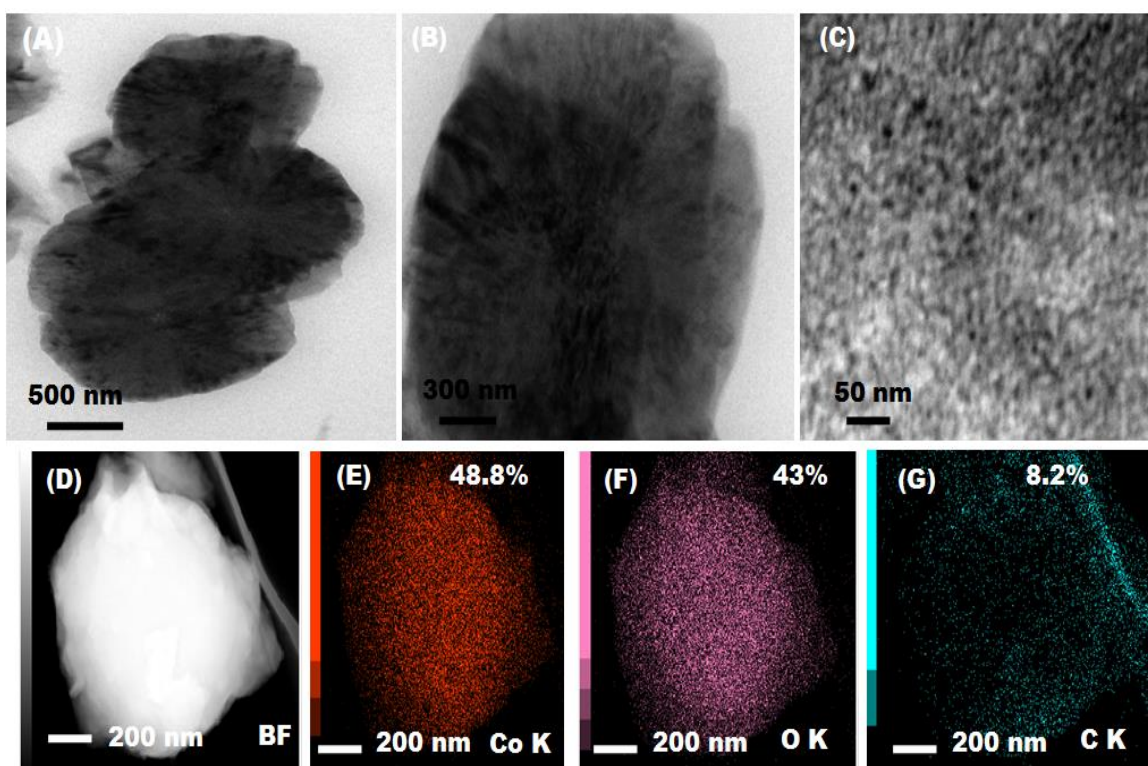


Figure 5. TEM and STEM-EDS mapping analyses of mesoporous composite C/Co₃O₄ micro-spherical flowers, (A–C) low and high magnification TEM micrographs, (D) bright filed STEM image, and (E–G) the corresponding elemental mapping showing the chemical composition of cobalt (E) oxygen (F), and carbon (G).

Thus, the enhanced mesoporosity features of the hierarchical flower-like structure would be contributable for efficient diffusion of fuel species and oxidants to the catalytically active sites of the electrode and can facilitate the ion/electron transport functionality leading to improve the utilization rate of electrode materials.

STEM-EDS analyses were further investigated to visualize the chemical composition of the elements of the hierarchical C/Co₃O₄ micro-spherical flowers as shown in Figure (Fig. 4D-G).

Although, a significant difference in the atomic distribution of the existed elements was evident, the corresponding distribution patterns of Co, C and O reveal that all elements were homogenously distributed throughout the formed heterostructure.

3.4 surface area and porosity properties

The electrochemical performances of the catalytic material were significantly influenced by the surface area and pore sizes. To clearly define the porous structure of the introduced C/Co₃O₄ micro-spherical flowers, N₂ adsorption/desorption analyses were carried out as shown in Fig. 6. The N₂ isotherm shows a distinct hysteresis loop in the relative pressure range (P/P_0) from 0.36-1. The corresponding specific surface areas were found to be 85.7 and 60.3 m² g⁻¹ for C/Co₃O₄ and Co₃O₄, respectively. The pore size distribution was analyzed by NLDFT and mainly centered at 4.69 and 8.77 nm for C/Co₃O₄ and Co₃O₄, respectively. Results show that the majority of the observed pores of the composite C/Co₃O₄ were fully located in the optimal mesoporous range which is favorable for efficient diffusion of reactants through the electrode [39]. The large surface area as well as the developed mesoporous structure of the hybrid C/Co₃O₄ micro-spherical flowers is beneficial for electrocatalytic reaction because these features provide rapid diffusion of electroactive species [39,40], facile shuttling of ions onto the mesopores matrices, and enhanced electrode/electrolyte contact.

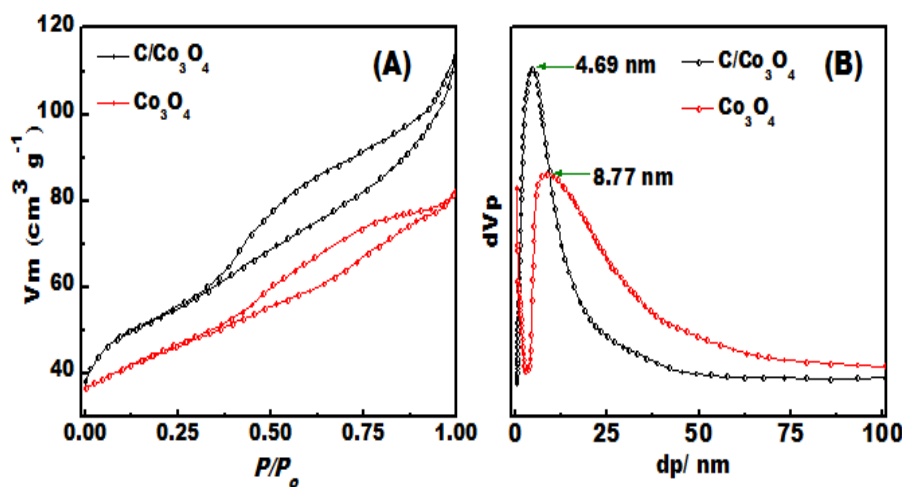


Figure 6. Textural properties of C/Co₃O₄ and C/Co₃O₄ measured by N₂-adsorption/desorption analyses; (A) N₂-isotherm obtained at 77K and (B) pore sizes distribution analysed by NLDFT.

3.5. Methanol electrooxidation

To further highlight the merits of our binder-free electrodes, the electrochemical performances of both Co_3O_4 and $\text{C}/\text{Co}_3\text{O}_4$ were evaluated in 0.5 M KOH solution as illustrated by the representative CV (Fig.7A). As shown, both electrodes reveal two pairs of redox peaks which can be attributed to the reversible transition of $\text{Co}^{2+}/\text{Co}^{3+}$ and $\text{Co}^{3+}/\text{Co}^{4+}$ reactions [41]. Interestingly, the integrated area of the hybrid $\text{C}/\text{Co}_3\text{O}_4$ electrode is significantly larger than that of naked Co_3O_4 electrode demonstrating the synergistic role of the carbon atoms which significantly enhance the electronic configuration of the hybrid and provide facile electron transport through the electrode surfaces.

The electrocatalytic activities for methanol oxidation on the binder free Co_3O_4 and $\text{C}/\text{Co}_3\text{O}_4$ electrodes were examined in 0.5 M KOH as presented in Fig.7B. With the addition of 0.5 M methanol, a sharp increase in the anodic current was observed in the forward scan indicating higher electroactivity of the hybrid electrode. It is further noteworthy that the current density at 0.6 V (vs. Hg/HgO) for the hybrid $\text{C}/\text{Co}_3\text{O}_4$ electrode is around three times higher than that for single Co_3O_4 .

Specifically, the electroactive CoOOH layer acts like electron trigger which efficiently facilitate the adsorption of methanol molecules and electron transfer to the catalytically active Co (IV) sites.

Simply, the oxidation mechanism of methanol at the $\text{C}/\text{Co}_3\text{O}_4$ electrode can be illustrated according to the following reactions [12].

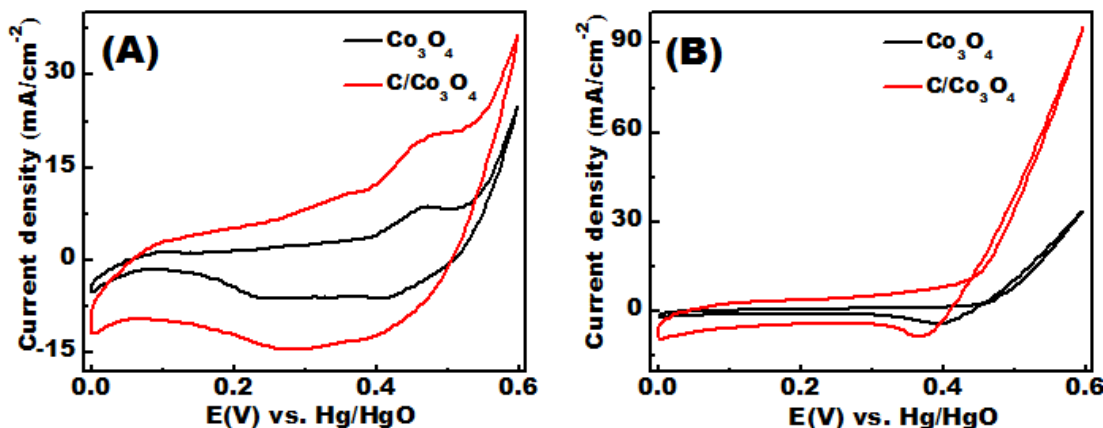
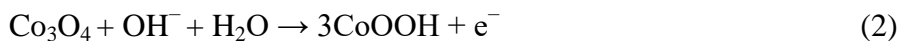


Figure 7. Electrochemical performances of $\text{C}/\text{Co}_3\text{O}_4$ and Co_3O_4 electrodes recorded in 0.5 M KOH solution at 50 mVs^{-1} without and with 0.5 M methanol. (A) CVs in 0.5 M KOH, (B) CVs in 0.5 M with 0.5 M methanol,

Others, the electrocatalytic activities of both bare NF and carbon modified NF (C/NF) toward methanol electrooxidation were probed as shown in Fig. 8. Our finding indicates that bare NF has a very poor electroactivity for methanol oxidation. Moreover, no significant change in the oxidation current was observed when the NF was modified with carbon nanoparticles (C/NF). The excellent

methanol electrooxidation property of the mesoporous C/Co₃O₄ electrode can be explained as follows: (i) the 3-D structure offer multifunctional features of short electron pathways and better utilization of the electrode material, (ii) the mesoporous structure with open spaces provide richer electroactive sites, rapid diffusion of methanol/electrolyte molecules to the inner mesopores leading to higher electrochemical performances [42], (iii) the direct growth of active material without conducting additives enable unique structure stability and ensure good mechanical adhesion and electrical connection to the current collector [43].

In addition, the absence of binders and polymeric additives can effectively boost the electrical conductivity and further hinder the electroactive sites blocking.

During the forward scan no anodic peak is observed which can be ascribed to the overlapping of oxygen evolution current and methanol oxidation current [44]. On the other hand, the peak observed at the reverse scan is mainly associated with the removal carbonaceous species like (i.e. carbon monoxide) that are not completely oxidized in the reverse scan.

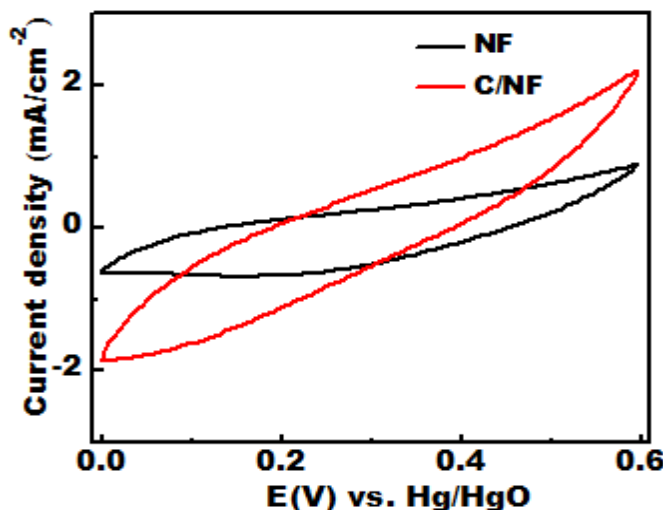


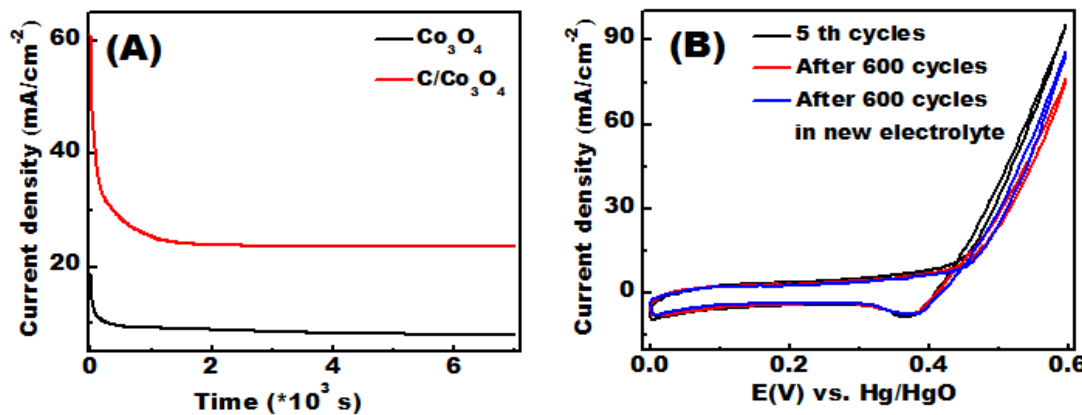
Figure 8. CVs of blank NF and C/NF electrodes recorded in 0.5 M KOH with 0.5 M methanol at a scan rate of 50 mV s⁻¹.

More importantly, the onset potential is a key parameter to assess the electroactivity materials. The highly positive onset potential of the transition metal oxides based electrodes is the main obstacle for broad utilization as electrocatalysts in fuel cells [12]. Significantly, the onset potential of the C/Co₃O₄ electrode is about 0.39 V (vs. Hg/HgO) which is much lower than that of single Co₃O₄ electrode (0.46 V (vs. Hg/HgO) indicating a better kinetic of methanol oxidation reaction at the hybrid electrode. Interestingly, the onset potential of our binder free C/Co₃O₄ electrode outperforms the previously reported NiCo₂O₄ [19], titanium-supported Ni nanoflakes [45] and NiO/multi-walled carbon nanotubes [46]. The low onset potential well evidenced the high electrocatalytic performance of the mesoporous C/Co₃O₄ hybrid.

The onset potential values of methanol oxidation obtained for various electroactive materials are presented in Table 1. As can be seen in the table, the onset potential of mesoporous C/Co₃O₄ is lower than that for the reported electrodes which demonstrate its improved catalytic activity towards methanol electrooxidation.

Table 1. The onset potentials recorded for various catalytic materials compared with that of C/Co₃O₄.

Sample	Onset potential (V)	fuel	reference
C/Co ₃ O ₄	0.39 (vs. Hg/HgO)	methanol	this study
Ni/graphite	0.43 (vs. Hg/HgO)	methanol	47
NiCo ₂ O ₄ /SS	0.42 (vs. Hg/HgO)	methanol	19
Co ₃ O ₄ /NiO	0.35 (vs. SHE)	methanol	12
NiCo ₂ O ₄ -rGO	0.4 (vs. Ag/AgCl)	methanol	48
NiCo ₂ O ₄	0.4 (vs. Hg/HgO)	methanol	49

**Figure 9.** (A) Current–time curves collected by CA technique (B) Long term stability test of C/Co₃O₄ electrode measured by normal CV under continuous potential cycling for 600 cycles in 0.5 M KOH with 0.5 M methanol at a scan rate of 50 mV s⁻¹.

Long term durability is an evoked parameter to maximize the practical application of electroactive materials. Herein, CA test was conducted at (0.55 V vs. Hg/HgO) for consecutive 7200 s to evaluate the stability of the electrode in the presence of 0.5 M methanol as shown in Fig. 9A. Clearly, the self supported electrodes exhibit an initial rapid current decay at the first 200 s which is mainly due to electrode poisoning by methanol intermediates and chemisorbed molecules [12]. Results show that the observed current density at the hybrid C/Co₃O₄ electrode is much higher than that of pristine Co₃O₄ electrode which is attributed to the unique structural stability due to the robust adhesion of the integrated structure to the porous substrate. Furthermore, the synergetic interaction between the Co species and the carbon matrices provide a stable structure.

The electrochemical stability of the proposed C/Co₃O₄ electrode was investigated by continuous potential cycling in 0.5 M KOH with 0.5 M methanol as displayed in Fig. 9B. As clearly seen, the current density of methanol electrooxidation at 0.6 V (vs. Hg/HgO) exhibits about 80% retention of the original value after 600 scan. Meanwhile, the current density recorded in a freshly

prepared electrolyte retained ~89.5% which could be ascribed to the activation and wettability of the electrode leading to improve the exposed electroactive surface area for electrochemical reactions.

Furthermore, the observed change in the oxidation current is attributed to the corresponding change in methanol concentration at the electrode active sites. Noticeably, the partial current decay after potential cycling is mainly attributed to the consumption of methanol around the electrode active sites. It is interesting to note that the oxidation current of the hybrid C/Co₃O₄ electrode after 600 cycles is still higher than that of naked Co₃O₄ electrode demonstrating the appreciable electrocatalytic activity of the C/Co₃O₄ for methanol oxidation. These findings illustrate that our suggested C/Co₃O₄ material hold a potential as a promising anodic electrode for high performance DMFCs.

The comparison of the electrochemical stability test carried out using continuous potential cycling compared with the recently reported precious metal free electrodes (Table 2). Results indicate the superior stability of the mesoporous C/Co₃O₄ hybrid electrode which is attributed to unique structural stability.

Table 2. Retained currents of methanol oxidation after continuous operation of the present C/Co₃O₄ electrode with respect to the reported literature.

Sample	Retention after long term stability	No. of cycles	fuel	reference
C/Co ₃ O ₄	89.5%	600	methanol	this study
NiCo ₂ O ₄	89%	500	methanol	[50]
NiCo ₂ O ₄	88% for NCO-NC	1000	methanol	[51]
NiCo ₂ O ₄ -rGO	79.3%	500	methanol	[48]
NiCo ₂ O ₄	72% and 75% with and without SDS, respectively	1000	methanol	[52]
NiCo ₂ O ₄	85%	500	methanol	[53]

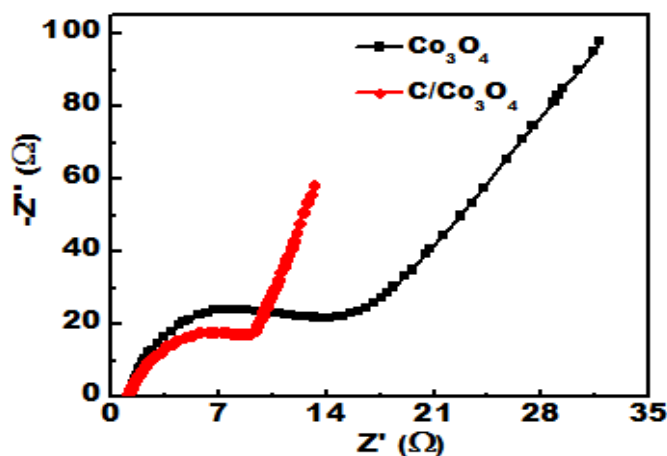


Figure 10. EIS measurement collected in 1 M KOH with 0.5 M methanol.

The charge transfer resistance of catalytic materials is an important factor to be evaluated. EIS measurements were investigated to show the enhanced performance of C/Co₃O₄ electrode. As depicted in Fig.10, the fitted Nyquist profiles of both C/Co₃O₄and pure Co₃O₄ electrodes are composed of high frequency semicircle and straight line in the low frequency which is ascribed to charge transfer resistance (Rct) and capacitive redox of Co₃O₄, respectively [2,19]. More importantly, the average diameter of the semicircle for C/Co₃O₄ is smaller than that of Co₃O₄. The slope of the straight line of C/Co₃O₄ is very small compared with that of pure Co₃O₄. Moreover, the composite electrode reveals an electrolyte resistance of 5.21 Ω which is lower than that of Co₃O₄ (10.75 Ω). These findings confirm fast electrons transfer to the active centers due to enhanced electronic features of the composite electrode.

It's well known that the electrooxidation process of methanol is very complicated and produce many oxidative compounds and intermediates and chemisorbed species. The complete oxidation of methanol leads to the production of 6 electrons. Methanol might react with the adsorbed water or hydroxyl species and produce CO₂ onto the electroactive sites. As schematically illustrated in Fig. 11, the methanol molecules were diffused inside the generated pores and open spaces of the self supported C/Co₃O₄ electrode and subsequently adsorbed at the active sites. The 3-D mesoporous porous structure of the electrode enables facile transport of ion and electron to active sites through the electrode which is beneficial for faster reaction kinetics. In addition, the electrochemical analyses show that our present C/Co₃O₄ electrode has a lower onset potential indicating that methanol could be a promising candidate as a cost-effective fuel for high performance fuel cells.

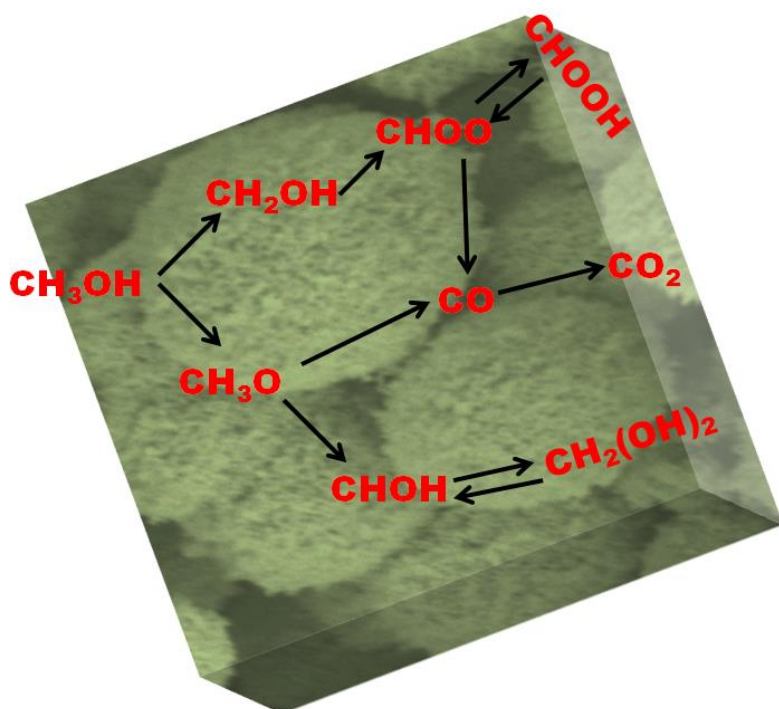


Figure 11. Schematic diagram illustrating the electrooxidation of methanol molecules at theC/Co₃O₄ electrode.

Based on the aforementioned discussion, the self supported mesoporous C/Co₃O₄ micro-spherical flowers heterostructures integrate different constituent into single electrode through the modification of each other in order to gain the favorable merits of both component and afford extraordinary properties leading to enhanced electro-catalytic reactivity. Therefore, the mesoporous C/Co₃O₄ synthesized directly on nickel substrate surfaces could be a feasible binder free electrode for direct methanol fuel cells.

5. CONCLUSION

In summary, we have developed one-pot microwave-assisted hydrothermal route followed by simple annealing treatment for the fabrication of C/Co₃O₄ in a vertical fashion to the underlying 3-D porous nickel foams. The carbon matrices were integrated within the nanostructure through the addition of thiourea across linking. The hybrid heterostructure integrate Co species and carbon framework into a single electrode to afford significant properties and gain the merits of both interacting components leading to improved electrocatalytic activity. The self supported mesoporous C/Co₃O₄ micro-spherical flowers show significantly improved electrocatalytic activity and excellent long-term stability towards methanol electrooxidation. The remarkable electrocatalytic performances of the C/Co₃O₄ micro-spherical flowers composite electrode can be attributed to the well-developed mesoporous structure with a large specific surface area which provides a facile ion/electron diffusion and better reaction kinetics. In addition, the improved conductivity and the direct contact to the current collector facilitate the electron transport and further ensure higher stability of the engineered structure. These results indicate that our scalable synthesis method can be extended to fabricate a novel class of efficient electroactive materials with a hierarchical mesoporous structure for practical application in energy storage and conversion devices.

ACKNOWLEDGEMENT

The authors would like to extend their sincere appreciation to the Dean ship of Scientific Research at King Saud University for its funding this Research Group NO. (RG1435-001).

References

1. A.S. Arico, P. Bruce, B. Scrosati, J.M. Tarascon, W. Van Schalkwijk, *Nat. Mater.*, 4 (2005) 366.
2. C. Liu, F. Li, L.P. Ma, H.M. Cheng, *Adv. Mater.*, 22 (2010) E28.
3. R. Ding, L. Qi, M. Jia, H. Wang, *Catal. Sci. Technol.*, 3 (2013) 3207.
4. Y. Lu, J.P. Tu, C.D. Gu, X.H. Xia, X.L. Wang, S.X. Mao, *J. Mater. Chem.*, 21(2011) 4843.
5. H. Wei, W. Jin, W. Erkang, *ACS Appl. Mater. Interfaces*, 6 (2014) 9481.
6. S. Chen, Z. Wei, X. Qi, L. Dong, Y.G. Guo, L. Wan, Z. Shao, L. Li, *J. Am. Chem. Soc.*, 134 (2012) 13252.
7. H.G. Sanchez-Casalongue, M.L. Ng, S. Kaya, D. Friebel, H. Ogasawara, A. Nilsson, *Angew. Chem. Int. Ed.*, 53 (2014) 7169.
8. Y. Lu, Y. Jiang, W. Chen, *Nano Energy*, 2 (2013) 836.
9. H.H. Wang, Z.H. Sun, Y. Yang, D.S. Su, *Nanoscale*, 5 (2013) 139.

10. H.P. Liu, J.Q. Ye, C.W. Xu, S.P. Jiang, Y.X. Tong, *J. Power Sources*, 177 (2008) 67.
11. S.J. Jiang, Y.W. Ma, G.Q. Jian, H.S. Tao, X.Z. Wang, Y.N. Fan, Y.N. Lu, Z. Hu, Y. Chen, *Adv. Mater.*, 21 (2009) 4953.
12. J.B. Wu, Z.G. Li, X.H. Huang, Y. Lin, *Journal of Power Sources*, 224 (2013) 1.
13. C. Jinbing, Y. Hailong, L. Yang, Q. Kangwen, H. Xiaoyi, X. Jinyou, H. Lei, L. Xianming, K.K. Jang, L. Yongsong, *J. Mater. Chem. A*, 3 (2015) 9769.
14. P.R. Jothi, K. Shanthi, G. Velayutham, *Journal of Power Sources*, 277 (2015) 350.
15. J. Xu, L. Gao, J. Cao, W. Wang, Z. Chen, *Electrochim. Acta.*, 56 (2010) 732.
16. Y. Liang, Y. Li, H. Wang, J. Zhou, J. Wang, T. Regier, H. Dai, *Nat. Mater.*, 10 (2011) 780.
17. J. Xiao, Q. Kuang, S. Yang, F. Xiao, S. Wang, L. Guo, *Sci. Rep.*, 3 (2013) 2300.
18. X.W. Xie, Y. Li, Z.Q. Liu, M. Haruta, W.J. Shen, *Nature*, 458 (2009) 746.
19. L. Qian, L. Gu, L. Yang, H. Yuan, D. Xiao, *Nanoscale*, 5 (2013) 7388.
20. Yoon, H. Taek, J. P. Yong, *Nanoscale research letters*, 7 (2012) 1.
21. M. Hasan, S. B. Newcomb, K. M. Razeeb, *J. Electrochem. Soc.*, 159 (2012) F203.
22. M. Chen, B. Wu, J. Yang, N. Zheng, *Adv. Mater.*, 24 (2012) 862.
23. X.H. Xia, J.P. Tu, Y.Q. Zhang, Y.J. Mai, X.L. Wang, C.D. Gu, X.B. Zhao, *RSC Adv.*, 2 (2012) 1835.
24. C.Z. Yuan, L. Yang, L.R. Hou, L.F. Shen, X.G. Zhang, X.W. Lou, *Energy Environ. Sci.*, 5 (2012) 7883.
25. X.H. Xia, J.P. Tu, Y.J. Mai, X.L. Wang, C.D. Gu, X.B. Zhao, *J. Mater. Chem.*, 21 (2011) 9319.
26. X. Xia, J. Tu, Y. Zhang, X. Wang, C. Gu, X.B. Zhao, H.J. Fan, *ACS Nano*, 6 (2012) 5531.
27. X. Xia, D. Chao, Z. Fan, C. Guan, X. Cao, H. Zhang, H.J. Fan, *Nano Lett.*, 14 (2014) 1651.
28. S. Laifa, C. Qian, L. Hongsen, Z. Xiaogang, *Adv. Funct. Mater.*, 24 (2014) 2630.
29. J. Kong, W. Liu, F. Wang, X. Wang, L. Luan, J. Liu, Y. Wang, Z. Zhang, M. Itoh, K.I. Machida, *J. Solid State Chem.*, 184 (2011) 2994.
30. L.X. Sheng, S.C. Jun, W.L. Xiong, C.Z. Hua, *Adv. Funct. Mater.*, 22 (2012) 861.
31. J. Wang, G. Du, R. Zeng, B. Niu, Z. Chen, Z. Guo, S. Dou, *Electrochimica Acta*, 55 (2010) 4805.
32. C.S. Park, K.S. Kim, Y.J. Park, *J. Power Sources*, 244 (2013) 72.
33. A.S. Aldwayyan, F.M. Al-Jekhedab, M. Al-Noaimi, B. Hammouti, T.B. Hadda, M. Suleiman, I. Warad, *Int. J. Electrochem. Sci.*, 8 (2013) 10506.
34. J. Jiang, L. Li, *Mater. Lett.*, 61 (2007) 4894.
35. H. C. Liu and S. K. Yen, *J. Power Sources*, 2007, 166, 478.
36. A.C. Ferrari, *Solid State Commun.*, 143 (2007) 47.
37. J. Liu, P. Chen, L. Deng, J. He, L. Wang, L. Rong, J. Lei, *Sci. Rep.*, 5 (2015) 15576.
38. F. Cao, R. Liu, L. Zhou, S. Song, Y. Lei, W. Shi, Zhao, F. Zhao, H. Zhang, *J. Mater. Chem.*, 20 (2010) 1078.
39. S.T. Mayer, R.W. Pekala, J.L. Kaschmitter, *J. Electrochem. Soc.*, 140 (1993) 446.
40. H. Jiang, J. Ma, C. Z. Li, *Chem. Commun.*, 48 (2012) 4465.
41. C. Zhou, Y. Zhang, Y. Li, J. Liu, *Nano Lett.*, 13 (2013) 2078.
42. J.D. Roy-Mayhew, G. Boschloo, A. Hagfeldt, I.A. Aksay, *ACS Appl. Mater. Interfaces*, 4 (2012) 2794.
43. P. Jiang, Q. Liu, Y. Liang, J. Tian, A. M. Asiri, X. Sun, *Angew. Chem., Int. Ed.*, 53 (2014) 12855.
44. J. Zhan, M. Cai, C. Zhang, C. Wang, *Electrochimica Acta*, 154 (2015) 70.
45. Q. Yi, W. Huang, J. Zhang, X. Liu, L. Li, *Catal. Commun.*, 9 (2008) 2053.
46. M. Asgari, M.G. Maragheh, R. Davarkhah, E. Lohrasbi, *J. Electrochem. Soc.*, 158 (2011) K225.
47. M.A. Abdel Rahim, R.M. Abdel Hameed, M.W. Khalil, *Journal of Power Sources*, 134 (2004) 160.
48. K.D. Ashok, K.L. Rama, H.K. Nam, J. Daeseung, H.L. Joong, *Nanoscale*, 6 (2014) 10657.
49. M. Yu, J. Chen, J. Liu, S. Li, Y. Ma, J. Zhang, J. An, *Electrochimica Acta*, 151 (2015) 99.

50. G. Li, Q. Lei, L. Ying, W. Yanyan, L. Jing, Y. Hongyan, X. Dan, *Journal of Power Sources*, 261, (2014) 317.
51. W. Wei, C. Qingxin, Z. Yingnan, Z. Wei, W. Xiaoyang, L. Xiaofeng, *New J. Chem.*, 39 (2015) 6491.
52. D. Rui, Q. Li, J. Mingjun, W. Hongyu, *Journal of Power Sources*, 251 (2014) 287.
53. Y.Y. Xin, Z.Y. Xian, L. Tao, J. Yong, H.L. Jin, J.H. Xing, *ACS Appl. Mater. Interfaces*, 6 (2014) 3689.

© 2016 The Authors. Published by ESG (www.electrochemsci.org). This article is an open access article distributed under the terms and conditions of the Creative Commons Attribution license (<http://creativecommons.org/licenses/by/4.0/>).